THE JOURNAL OF BIOLOGICAL CHEMISTRY VOL. 285, NO. 35, pp. 27251–27258, August 27, 2010

Biophysical Investigations of Complement Receptor 2 (CD21 and CR2)-Ligand Interactions Reveal Amino Acid Contacts Unique to Each Receptor-Ligand Pair*

Received for publication, January 21, 2010, and in revised form, May 18, 2010 Published, JBC Papers in Press, June 17, 2010, DOI 10.1074/jbc.M110.106617

James M. Kovacs[‡], Jonathan P. Hannan[§], Elan Z. Eisenmesser[¶], and V. Michael Holers[‡1]

From the Departments of [‡]Medicine and Immunology and [¶]Biochemistry and Molecular Genetics, University of Colorado Denver School of Medicine, Aurora, Colorado 80045 and the [§]Institute of Structural and Molecular Biology, University of Edinburgh, Edinburgh EH9 3JR, Scotland, United Kingdom

Human complement receptor type 2 (CR2 and CD21) is a cell membrane receptor, with 15 or 16 extracellular short consensus repeats (SCRs), that promotes B lymphocyte responses and bridges innate and acquired immunity. The most distally located SCRs, SCR1–2, mediate the interaction of CR2 with its four known ligands (C3d, EBV gp350, IFNα, and CD23). To ascertain specific interacting residues on CR2, we utilized NMR studies wherein gp350 and IFNα were titrated into ^{15}N-labeled SCR1–2, and chemical shift changes indicative of specific intermolecular interactions were identified. With backbone assignments made, the chemical shift changes were mapped onto the crystal structure of SCR1–2. With regard to gp350, the binding region of CR2 is primarily focused on SCR1 and the inter-SCR linker, specifically residues Asn^{11}, Arg^{13}, Ala^{22}, Arg^{28}, Ser^{32}, Arg^{36}, Lys^{41}, Lys^{57}, Tyr^{64}, Lys^{67}, Tyr^{68}, Arg^{83}, Gly^{84}, and Arg^{89}. With regard to IFNα, the binding is similar to the CR2-C3d interaction with specific residues being Arg^{13}, Tyr^{16}, Arg^{28}, Ser^{42}, Lys^{48}, Lys^{50}, Tyr^{68}, Arg^{83}, Gly^{84}, and Arg^{89}. We also report thermodynamic properties of each ligand-receptor pair determined using isothermal titration calorimetry. The CR2-C3d interaction was characterized as a two-mode binding interaction with K_d values of 0.13 and 160 μM, whereas the CR2-gp350 and CR2-IFNα interactions were characterized as single site binding events with affinities of 0.014 and 0.035 μM, respectively. The compilation of chemical binding maps suggests specific residues on CR2 that are uniquely important in each of these three binding interactions.

Human complement receptor 2 (CR2/CD21) is a 145-kDa transmembrane protein comprised of 15 or 16 short consensus repeat (SCR)[2] extracellular domains, a 28-amino acid single pass transmembrane domain, and a short 34-amino acid intracellular domain (1–5). Each of the extracellular SCRs includes ~60–70 amino acid residues, and each is connected by linker regions of 3–8 amino acid residues. All SCRs contain a number of conserved residues, including four cysteine residues, which form a pattern of disulfide bridges connecting Cys^1–Cys^3 and Cys^2–Cys^4. CR2 is primarily present on B cells, where it is found in complex with other membrane proteins that promote normal humoral and cellular immune responses (6–9). Using the most distally located SCR domains, SCR1–2, CR2 ligates four classes of ligands, complement component 3 proteolytic fragments iC3b, C3dg, and C3d (10, 11); the Epstein-Barr virus (EBV) glycoprotein gp350/220 (gp350) (12–14); the low affinity IgE receptor CD23 (15, 16); and the cytokine interferon α (IFNα) (17–19).

The primary role of CR2 is to function as a B cell co-receptor for antigen-mediated B cell activation through enhanced signal transduction (20, 21). This function is carried out through co-ligation via C3d and surface IgM, where C3d is covalently attached to an antigen (22–28). CR2 is also the obligate cellular receptor for EBV through its envelope surface glycoprotein gp350 (12, 20, 29–31). Actual cellular EBV infection is achieved after the ligation of CR2 to gp350 presumably tethers the virus close enough to the cell surface (14, 32, 33), allowing viral gp42 to bind human leukocyte antigen class II molecules (34, 35) and subsequently triggering host cell fusion via three additional viral glycoproteins gB, gH, and gL (36–38). IFNα has been shown to be a ligand of CR2, although the physiologic importance of this interaction remains unclear (17–19). It has been suggested, however, that IFNα and CR2 may be involved in the development of the autoimmune disease systemic lupus erythematosus (39–41).

Mutagenesis studies along with structural studies of the CR2-gp350 interaction have suggested residues on CR2 that are required for the interaction (20, 42, 43). ELISA and flow cytometry were used to test candidate CR2 mutants for the binding of gp350 and CR2 (20, 42, 43). In recent studies, specific residues on CR2 that were found to have a deleterious effect on gp350 binding when mutated included Arg^{13}, Ser^{15}, Arg^{28}, Arg^{36}, Lys^{41}, Lys^{57}, Lys^{67}, Arg^{83}, and Arg^{89} (42, 43). In separate work, residues Pro^8–Ser^{15} within the first conserved inter-cysteine region of SCR1 and the linker region between SCR1 and SCR2 were highlighted as being essential for gp350 binding to occur (20). These data, in conjunction with separate mutagenesis analyses targeting the gp350 molecule, were used to drive an *in silico* model of the CR2-gp350 interaction utilizing the soft docking program HADDOCK (43–45). This analysis suggested

* This work was supported, in whole or in part, by National Institutes of Health Grant R0-1 CA053615 (to V. M. H.). This work was also supported by an American Heart Association predoctoral fellowship (to J. M. K.) and assisted by the University of Colorado Denver-Rocky Mountain Regional 900 MHz Facility.

[1] To whom correspondence should be addressed: 1775 Aurora Ct., M20-3102E Mail Stop B115, Aurora, CO 80045. Tel.: 303-724-7605; Fax: 303-724-7581; E-mail: michael.holers@ucdenver.edu.

[2] The abbreviations used are: SCR, short consensus repeat; ITC, isothermal titration calorimetry.

that the primary interaction on CR2 was between SCR1 and the linker region joining SCR1 to SCR2 and the linker region between domain 1 and domain 2 for gp350 (43).

CR2 has been suggested as a receptor for IFNα by the finding that IFNα mimics both gp350 and C3d binding, and the observation that all three ligands bind a similar region on CR2 (18, 19). The mimicry was shown to be functional as well (18). After both C3d and IFNα structures were solved, the putative CR2 binding sequence was found to have similar structural motifs. IFNα has been described as being able to bind to multiple forms of CR2 from full length to SCR1–2, although to varying degrees (17). Although CR2 has been shown to be a receptor for IFNα, the IFNα-binding site within CR2 SCR1–2 is unknown.

To further study the ligand-specific differential binding to CR2, we have employed NMR chemical shift analysis during ligand titrations to identify specific residues involved in the CR2-gp350 and CR2-IFNα interactions. Furthermore, we have used ITC to measure thermodynamic binding constants for the CR2-C3d, CR2-gp350, and CR2-IFNα interactions. The results from the experiments carried out suggest that each CR2 ligand interaction utilizes unique residues within SCR1, SCR2, and the inter-SCR linker region.

EXPERIMENTAL PROCEDURES

Expression and Purification of Recombinant Proteins—Human CR2 SCR1–2 for NMR and ITC studies was expressed in *Pichia pastoris* using a BioFlo 110 fermentor (New Brunswick Scientific, Edison, NJ) as described previously (46). Briefly, a single colony was grown in 5 ml of *Pichia* basal salt medium containing 1% glycerol (BMG) overnight at 30 °C, 250 rpm, expanded to 50 ml of BMG (24 h), and finally expanded to 300 ml of BMG (24 h). The inoculation culture was centrifuged at 2500 × *g* at 25 °C and resuspended in 30 ml of BMG. The 30-ml inoculation culture was used to inoculate 1 liter of minimal *Pichia* basal media containing 40 g of glycerol. Dissolved O_2 concentration was maintained at 40% with the temperature at 30 °C and pH 5.0 using 2 M KOH. Initial feeds were batch glycerol feeds; transition to methanol was eased by a methanol injection before an exponential methanol feed profile was initiated. Methanol induction lasted for 2 days, after which the culture was centrifuged to remove cellular debris. The supernatant was exchanged into 10 mM formate, pH 4.0, before being passed over an SP-Sepharose column (2 × 5-ml SP HiTrap columns, GE Healthcare) followed by a CR2 affinity column, generated in-house by binding GST-C3d to a GSTrap column (GE Healthcare). CR2 was eluted with an increasing linear NaCl gradient, 0–1.0 M in ⅓× phosphate-buffered saline (PBS: 1.6 mM $MgCl_2$, 0.9 mM KCl, 0.5 mM KH_2PO_4, 45.6 mM NaCl, 2.7 mM Na_2HPO_4, pH 7.4). Finally, CR2 SCR1–2 was purified by size exclusion chromatography. Purity and identity of CR2 were monitored via SDS-PAGE, Western blot analysis, and mass spectrometry. Both ^{15}N and ^{15}N-^{13}C isotopically labeled proteins were prepared using this strategy. For ^{15}N isotopically labeled CR2, [^{15}N]ammonium sulfate was used. For ^{15}N-^{13}C isotopically labeled CR2, [^{15}N]ammonium sulfate, [^{13}C]glycerol, and [^{13}C]methanol were used. Isotopically enriched chemicals were purchased from Isotec Inc., Miamisburg, OH.

Human CR2 SCR1–2 for ITC studies was generated using the pMAL-P2X expression system in *Escherichia coli* as described previously (42, 43). Ampicillin-resistant colonies were used to start overnight cultures that were expanded to 1 liter and grown at 37 °C until an A_{600} of 0.3 was obtained. Cultures were induced with 0.3 mM isopropyl β-D-thiogalactoside at 30 °C overnight before harvesting by centrifugation. Harvested pellets were resuspended in amylose column buffer (20 mM Tris-HCl, pH 7.4, 0.2 M NaCl, 1 mM EDTA) and lysed by sonication. Lysate was clarified by centrifugation and applied to an amylose resin column (New England Biolabs, Ipswich, MA). Bound MBP-CR2 SCR1–2 was eluted from the column using amylose column elution buffer (amylose column buffer plus 10 mM maltose). Finally, the MBP-CR2 SCR1–2 was purified by size exclusion chromatography. Purity and identity of MBP-CR2 were monitored via SDS-PAGE and Western blot analysis.

Human C3d for ITC studies was generated using the pGEX expression system in *E. coli* as described previously (47). Briefly, ampicillin-resistant colonies were used to start overnight cultures that were expanded to 1 liter and grown at 37 °C until an A_{600} of 0.3 was achieved. Cultures were induced with 0.3 mM isopropyl β-D-thiogalactoside at 30 °C overnight before harvesting by centrifugation. Harvested pellets were resuspended in GST column buffer (50 mM Tris-HCl, pH 8.0, 250 mM NaCl, 1 mM EDTA) and lysed by sonication. Lysate was clarified by centrifugation and applied to a GStrap column (GE Healthcare). C3d was cleaved from the column by digesting with 50 units of thrombin overnight at 4 °C and subsequently purified by size exclusion chromatography. Purity of C3d was monitored via SDS-PAGE.

Purification of a truncated construct of EBV gp350 comprising residues 1–470 of the wild-type protein for NMR titrations and ITC studies was completed as described previously (46). gp350 was produced by infecting Sf9 insect cells with the gp350-packaged baculovirus particles (pVI-Bac Transfer vector, C-terminal polyhistidine tag) at a multiplicity of infection of 3. The baculoviral supernatant was concentrated, buffered with 10 mM Tris-HCl with 10 mM imidazole, pH 7.4, and applied to a 5-ml HiTrap column (GE Healthcare) and subsequently eluted with a linear imidazole gradient. Purity and identity of gp350 were monitored via SDS-PAGE and Western blot analysis.

Human IFNα for NMR titrations and ITC studies was generated using the pMAL expression system in *E. coli* as described previously (48). Ampicillin-resistant colonies were used to start overnight cultures that were expanded to 1 liter and grown at 37 °C until an A_{600} of 0.3 was obtained. Cultures were induced with 0.3 mM isopropyl β-D-thiogalactoside at 25 °C overnight before harvesting by centrifugation. Harvested pellets were resuspended in amylose column buffer (20 mM Tris-HCl, pH 7.4, 0.2 M NaCl, 1 mM EDTA) and lysed by sonication. Lysate was clarified by centrifugation and applied to an amylose resin column (New England Biolabs). Bound MBP-IFNα was eluted from the column using amylose column elution buffer (amylose column buffer plus 10 mM maltose). After elution, the maltose-binding protein tag was cleaved overnight at 4 °C with Factor Xa (New England Biolabs). Finally, IFNα was purified by size

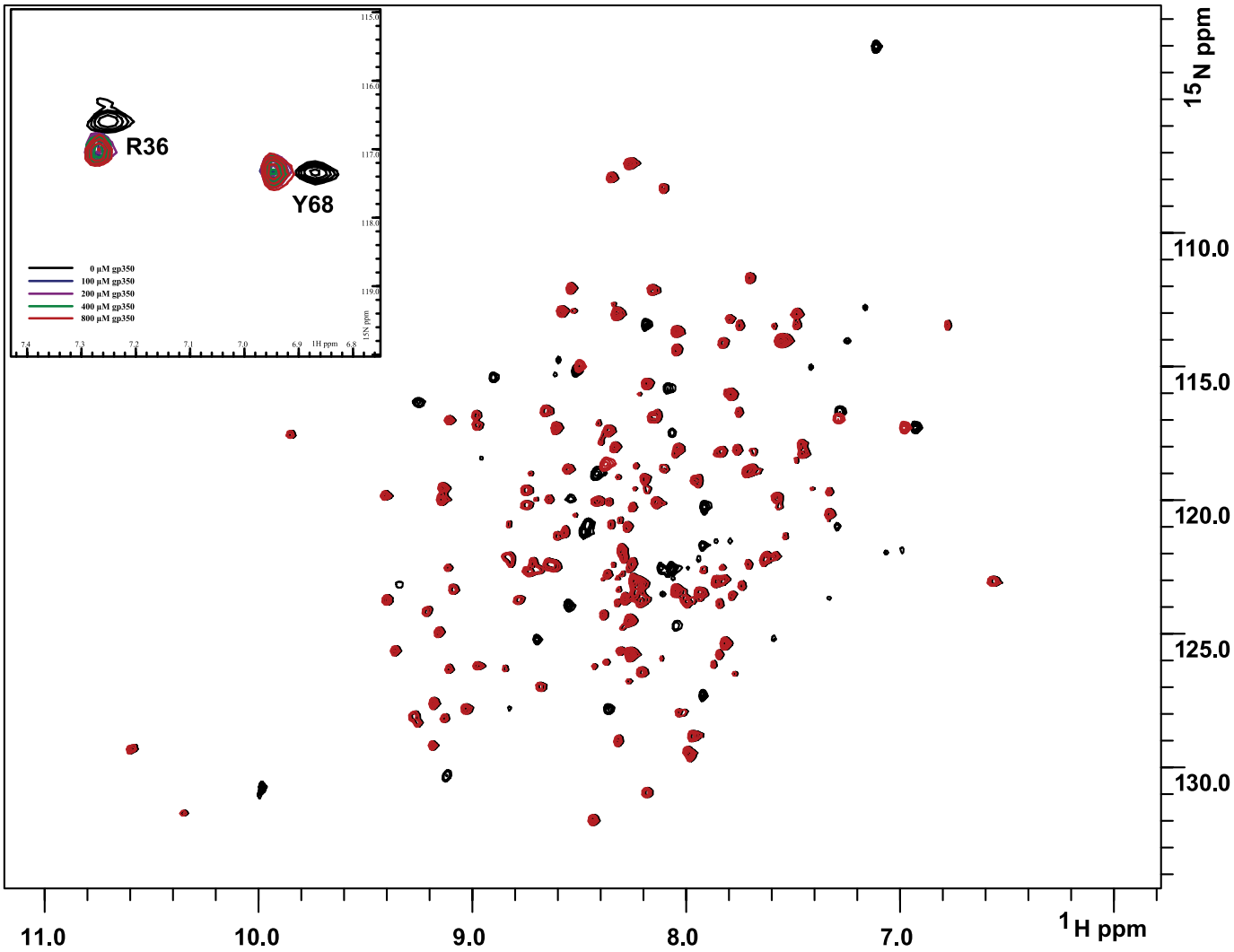

FIGURE 1. **NMR titration analysis reveals that SCR1 and SCR2 of CR2 are both involved in ligating gp350.** Two superimposed ^{1}H-^{15}N TROSY-HSQC spectra of ^{15}N-labeled CR2 SCR1–2 (0.6 mM in 1/3× PBS) were collected during titration with increasing amounts of gp350. *Black*, no gp350; *red*, saturating amounts of gp350. *Inset*, detailed view of chemical shift change. The numbering scheme used here for CR2 is based on the amino acid sequence for the mature protein.

exclusion chromatography. Purity and identity of IFNα were monitored via SDS-PAGE and Western blot analysis.

NMR Analysis—NMR experiments were carried out on Varian 600, 800, and 900 MHz magnets housed in the Rocky Mountain Regional NMR Facility at the University of Colorado Denver School of Medicine campus (600 and 900 MHz) and in the W. M. Keck High Field NMR Facility at the University of Colorado Boulder campus (800 MHz). The uniformly ^{15}N-^{13}C-labeled SCR1–2 domains of CR2 in 1/3× PBS were used to sequentially assign the ^{15}N-TROSY-HSQC (49) by using HNCACB (50), CBCA(CO)NH (51), and ^{15}N-edited NOESY-HSQC (52) three-dimensional spectra. The NMR data were processed with nmrPipe (53) and analyzed with ccpNMR (54). Chemical shift changes were monitored using ccpNMR by overlaying TROSY-HSQC spectra from free CR2 SCR1–2 and CR2 SCR1–2 with increasing concentrations of either EBV gp350 or IFNα.

ITC Analysis—ITC experiments were carried out on a Microcal VP-ITC housed in the Biophysics Core Facility on the University of Colorado Denver School of Medicine campus. CR2 SCR1–2 in 1/3× PBS was used in titration experiments carried out at 20 °C. Each titration experiment consisted of a 5-μl injection followed by 26 injections of 10 μl of graded concentrations of C3d, gp350, or IFNα. Data were analyzed using the software provided by the manufacturer (Origin, version 7.0, MicroCal) using either single site or two-site binding models (55).

RESULTS

Chemical Shift Analysis—Using previously described resonance assignments (48), full-length ligands EBV gp350 and IFNα were titrated into uniformly ^{15}N-labeled CR2 SCR1–2 samples, and the ^{1}H-^{15}N chemical shifts were monitored (Figs. 1–3). Titration with EBV gp350 yielded a single mode of binding characterized by the disappearance and reappearance of specific resonances, indicative of a tight interaction. The residues on CR2 SCR1–2 exhibiting chemical shift changes are Asn^{11}, Arg^{13}, Ala^{22}, Arg^{28}, Ser^{32}, Arg^{36}, Lys^{41}, Lys^{57}, Tyr^{64}, Lys^{67}, Tyr^{68}, Arg^{83}, Gly^{84}, and Arg^{89}. These residues encompass the SCR1, SCR2, and the inter-SCR linker region of CR2 (Figs. 3 and 4*A*). Chemical shift change magnitudes are shown in Fig. 3.

These results suggest that the inter-SCR linker and a ridge on SCR1 play the most important role in ligating gp350 to CR2 (Fig. 4*A*). Because this interaction is under slow exchange on the NMR time scale, only an upper limit K_d value can be calculated. The K_d value was calculated using the minimal observed chemical shift difference between free and bound resonances (about 60 Hz); assuming a diffusion-limited on-rate of $\sim 10\times 8$ M^{-1} s^{-1}, an upper limit to the binding constant was calculated as ~60 μM (Table 1).

Full-length IFNα was also titrated into uniformly ^{15}N-labeled CR2 SCR1–2 samples, and the ^{1}H-^{15}N chemical shifts were monitored (Fig. 2). Titration with the cytokine IFNα yielded a single mode of binding similar to that of gp350 ligation and thus a tight interaction. The residues on CR2 SCR1–2 exhibiting chemical shift changes are Arg^{13}, Tyr^{16}, Arg^{28}, Ser^{42}, Lys^{48}, Lys^{50}, Tyr^{68}, Arg^{83}, Gly^{84}, and Arg^{89}. These residues encompass the SCR1, SCR2, and the inter-SCR linker region of CR2 (Figs. 3 and 4*B*). Chemical shift change magnitudes are shown in Fig. 3. These results suggest that IFNα-binding surface is similar to that of the C3d-binding surface (Fig. 3). Similar to the gp350 chemical shift changes, the chemical shift changes for the IFNα suggest tighter than visible via the NMR time scale; the upper limit K_d was calculated as before to be ~70 μM (Table 1).

For comparison, we have illustrated unique and shared residues on CR2 required for ligation by C3d, gp350, and IFNα (Fig. 4*C*). In addition, we have also shown an overlay of chemical shift change magnitudes for each ligation state (Fig. 3).

Thermodynamics of CR2-Ligand Interactions—ITC was used to determine binding affinities of CR2-ligand interactions. Consistent with the NMR chemical shift analyses, the interaction between CR2 and C3d was determined to be a two-site binding based on the goodness of fit of a two-site binding model rather than a single site binding model. The two affinities are 0.13 ± 0.05 and 160 ± 20 μM. The interaction between CR2 and gp350 was fit using a single site binding model that yielded an affinity of 0.014 ± 0.009 μM. The interaction between CR2 and IFNα was fit using a single site binding model yielding an affinity of 0.035 ± 0.008 μM. The results of all thermodynamic parameters from NMR- and ITC-derived affinities can be found in Table 1.

TABLE 1

CR2 binding constants from NMR titrations and ITC

Shown are weak and upper limits to tight binding constants for CR2-ligand interactions determined using NMR titrations monitoring chemical shift changes. Also shown are CR2-ligand binding constants determined using ITC. UL, upper limit.

CR2 ligand	NMR determined, K_d	ITC determined, K_d
	μM	μM
C3d	Tight, UL 45	0.13 ± 0.05
	Weak 130 ± 60	160 ± 20
gp350	UL, 60	0.014 ± 0.009
IFN-α	UL, 70	0.036 ± 0.008

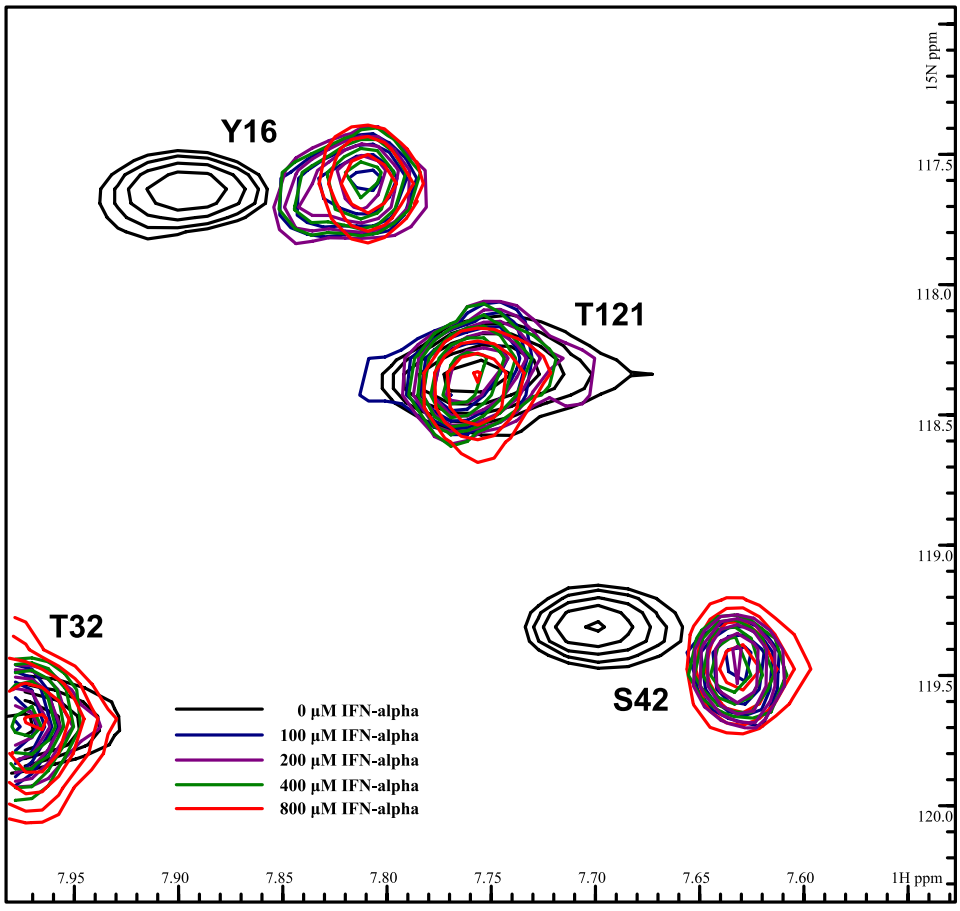

FIGURE 2. **NMR titration analysis reveals that SCR1 and SCR2 of CR2 are both involved in ligating IFNα.** Five superimposed ^{1}H-^{15}N TROSY-HSQC spectra of ^{15}N-labeled CR2 SCR1–2 (0.6 mM in 1/3× PBS) were collected during titration with increasing amounts of IFNα. *Black*, no IFNα; *blue*, with 100 μM IFNα; *purple*, with 200 μM IFNα; *green*, with 400 μM IFNα; *red*, with 800 μM IFNα.

DISCUSSION

Here, we have utilized a 2-fold approach to study CR2-ligand interactions in the fluid phase. First, we have used NMR spectroscopy to elucidate residues on SCR1–2 that interact with either gp350 or IFNα. This was accomplished by titrating full-length gp350 or IFNα into ^{15}N-labeled CR2 SCR1–2 and monitoring chemical shifts. Second, we utilized ITC to further characterize and determine binding constants for each CR2-ligand interaction. This body of data builds on our previous NMR binding map of the CR2-C3d interaction and increases the knowledge of the thermodynamic and physicochemical properties of the individual binding interactions.

Earlier studies that were aimed at determining areas of CR2 that interacted with gp350 began with complete SCR deletion mutations to determine which SCR domains were required for interaction with gp350. It was shown that both SCR1 and -2 were needed for the binding of gp350 (1, 12, 20, 56, 57). Further-

more, it was also reported that specific areas of SCR1–2 were important in binding gp350 (20, 58). These areas were between the first and second and the second and third cysteine residues of SCR1 and the second half of SCR2; the amino acids included Arg^{89} to Arg^{96} and Thr^{100} to Ser^{128} in SCR2 (58). Interactions with the linker were also inferred by the finding that the introduction of a glycosylation site into the linker eliminated gp350 but not C3d binding (20, 31, 57).

More recently, it has been shown that there are specific interacting amino acids on the surface of CR2 SCR1–2. Mutagenesis studies suggested that residues Arg^{13}, Ser^{15}, Arg^{28}, Arg^{36}, Lys^{41}, Lys^{56}, Lys^{67}, Arg^{83}, and Arg^{89} are the most important residues in the CR2-gp350 interaction (42, 43). In addition, using HADDOCK, a model of interaction was determined where the linker region between domains one and two of gp350 interacts with the linker between SCR1 and SCR2 of CR2 (43).

However, although there have been suggestions of important regions and more recently amino acids that are important in the interaction between CR2 and gp350, there has been no physical evidence of these interactions occurring. We now present a CR2 binding map that illustrates residues important to the CR2-gp350 interaction (Fig. 4*A*). Residues determined to be important to the CR2-gp350 interaction are Asn^{11}, Arg^{13}, Ala^{22}, Arg^{28}, Ser^{32}, Arg^{36}, Lys^{41}, Tyr^{64}, Lys^{67}, Tyr^{68}, Arg^{83}, Gly^{84}, and Arg^{89}. Because there are multiple interactions within the linker region, it is possible to imagine a rearrangement of SCR domains about the linker region upon binding gp350 and thus allowing for all contact points to be met. It is important to keep in mind that some of these residues deemed as important for interaction might be important in structural rearrangement upon binding and not intimate amino acid contact sites. Some resonances disappear due to the large size of the ligated complex, ~110 kDa, and the resultant increased tumbling time; therefore, alternative labeling techniques are necessary to observe such resonances.

Our data suggest that the linker region is important in the CR2-gp350 interaction. The linker interaction has been shown to be important in mutagenesis-derived data as well as in the soft dock model from HADDOCK (43). The linker region between SCR1 and SCR2 is eight amino acids, one of the longest in SCR-containing proteins, and thus

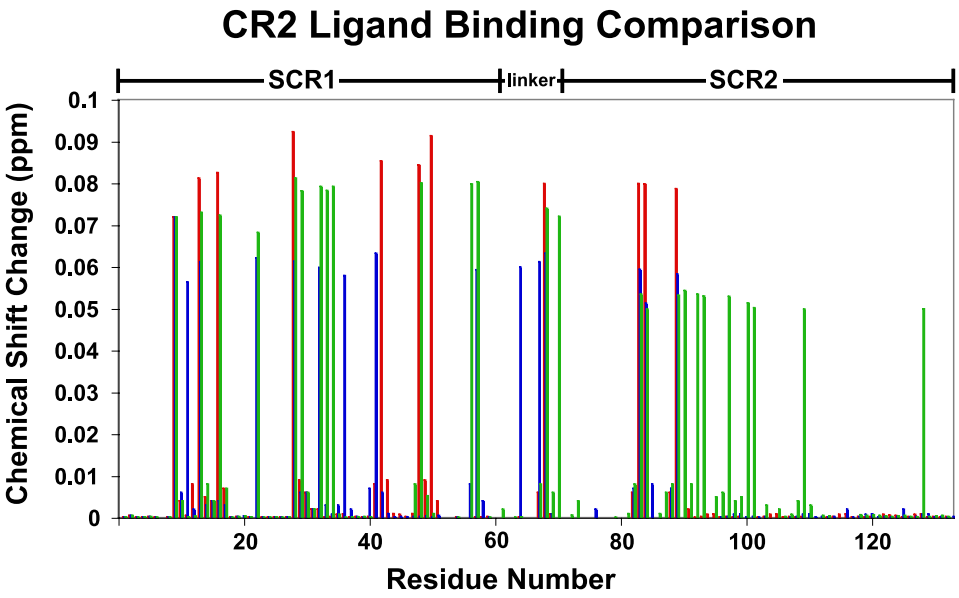

FIGURE 3. **NMR-derived CR2-ligand binding residue comparison.** *Histogram* illustrates chemical shift changes induced in the backbone amides of CR2 SCR1–2 upon binding C3d, IFNα, or gp350. Residues affected by C3d ligation are illustrated in *green*. Residues affected by IFNα ligation are illustrated in *blue*. Residues affected by gp350 ligation are illustrated in *red*.

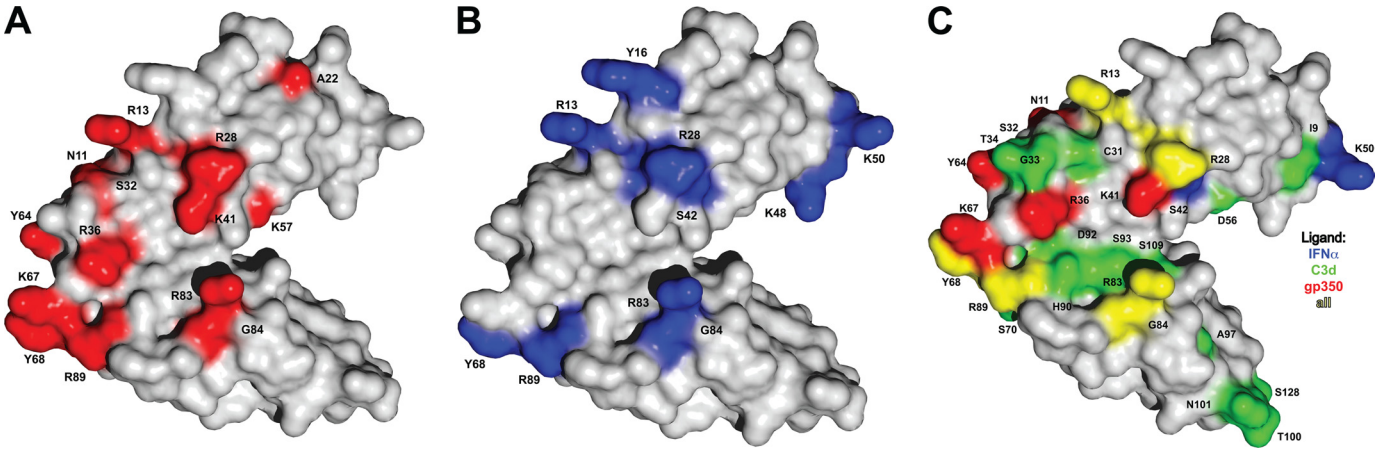

FIGURE 4. **Surface representation of CR2 SCR1–2 x-ray crystal structure in its ligand-bound state (C3d not shown) with NMR-determined ligand binding residues.** *A,* NMR-determined gp350-binding residues. *Gray* residues represent residues unaffected by gp350 titration. The *red* residues on SCR1, the linker region, and SCR2 represent residues involved in gp350 binding to CR2 SCR1–2. *B,* NMR-determined IFNα-binding residues. *Gray* residues represent residues unaffected by IFNα titration. The *blue* residues on SCR1, the linker region, and SCR2 represent residues involved in IFNα binding to CR2 SCR1–2. *C,* unique and shared binding residues of CR2-ligand interaction determined by NMR. *Gray* residues represent residues either unaffected by ligand binding or affected in two out of three of the ligand binding events. The *blue* residues represent residues that are uniquely involved in CR2 binding to IFNα. The *red* residues represent residues that are uniquely involved in CR2 binding to gp350. The *green* residues represent residues that are uniquely involved in CR2 binding to C3d. The *yellow* residues represent residues that are involved in all three CR2 ligand binding events.

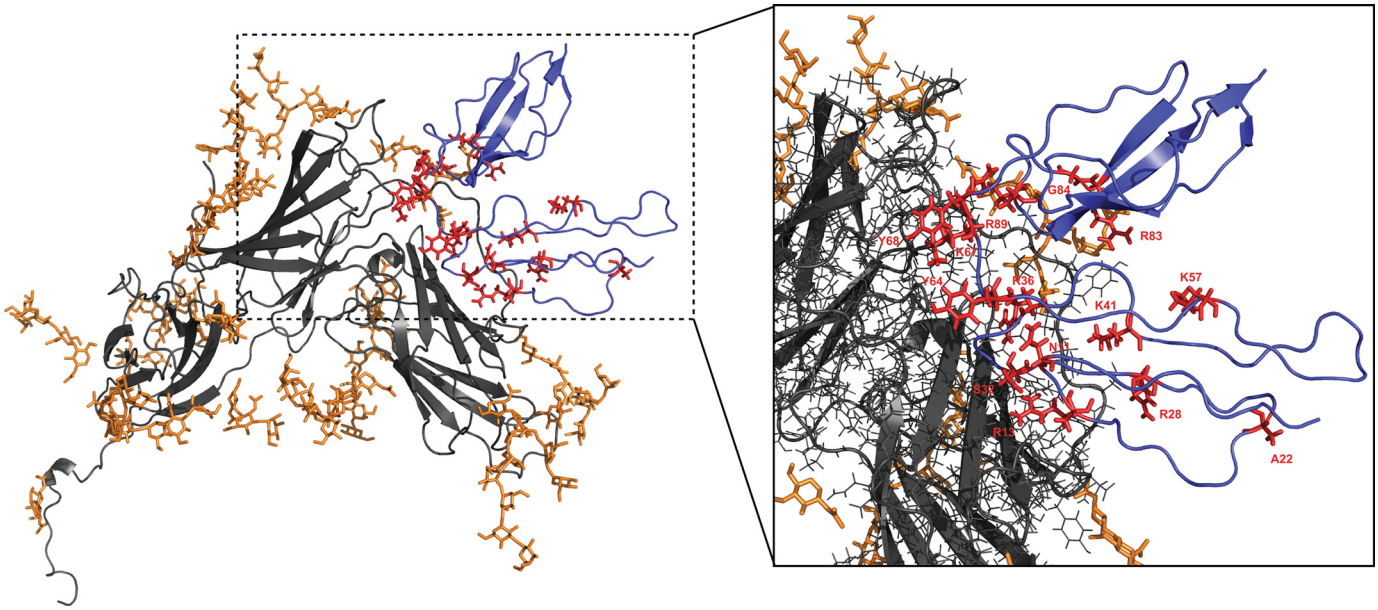

FIGURE 5. **HADDOCK CR2-gp350 docking model with NMR-derived CR2-gp350 ligand binding residues highlighted.** Model is from Young *et al.* (43). *Gray ribbons* represent gp350, and *orange* represents glycosyl groups that decorate the surface of gp350. *Blue ribbons* represent CR2 SCR1–2 with NMR-derived CR2-gp350 ligand-binding residues in *red*. *Inset*, magnified view of theoretical side chain interactions between NMR-derived binding residues and gp350 mapped on the docking model of Young *et al.* (43).

it is likely to be flexible enough to mediate multiple ligand interactions. Unlike the CR2-C3d interaction, our data suggest that two residues in the linker region, Lys^{67} and Tyr^{68}, are important in the CR2-gp350 interaction. Thus, with both a charged residue, Lys^{67}, and a hydroxyl-containing residue, Tyr^{68}, it is likely that the interaction with the linker is stronger in the CR2-gp350 interaction than with the CR2-C3d interaction, a start to defining how CR2 can mediate multiple ligand interactions.

As with the CR2-C3d interaction (59, 60), the CR2-gp350 interaction is likely driven largely by electrostatic interactions as is evident by the large number of charged residues that we have determined to be important in the CR2-gp350 interaction. The majority of these charged residues are found on SCR1, suggesting that this domain plays a more significant role in the CR2-gp350 interaction. Interestingly, Arg^{83} was also determined to be important in the CR2-gp350, without many other residues around Arg^{83} as found to exhibit changes in chemical shift during the CR2-C3d interaction. These data, along with the weak interaction found in the CR2-C3d interaction, could signify that the Arg^{83} interaction is more important in the initial electrostatic attraction of gp350 to CR2 than to significant amino acid contacts. The charged residues that were determined in this study overlap well with the previous mutagenesis study and consequently agree with the HADDOCK model (42, 43). Again, as with the CR2-C3d NMR binding map, we have found that there are more residues than just charged residues involved in the CR2-gp350 interaction. Specifically, several hydroxyl-containing amino acids (Ser^{32}, Tyr^{64}, and Tyr^{68}) are important in the CR2-gp350 interaction. These side chain interactions are likely hydrogen bond interactions. As the new data suggest, the CR2-gp350- and CR2-C3d-binding sites are likely similar, which explains why the ligands cross-compete, yet there are substantial differences that begin to explain how selective binding occurs.

The HADDOCK model fits well with the NMR-determined CR2-gp350-binding residues (Fig. 5). All but two residues, Lys^{57} and Ala^{22}, are found within the hypothetical binding face derived from the HADDOCK model. The Ala^{22} chemical shift is likely due to a slight conformational change in SCR1 upon CR2 binding gp350. The Lys^{57} interaction described by NMR could be used to drive a different and potentially lower energy docking model, as this residue was not utilized as an active residue in the simulated docking approach of Young *et al.* (43).

The CR2-IFNα interaction has been characterized in several ways. The first started with investigating sequence similarities between proposed CR2-binding sites on C3d and gp350 (19). To further confirm the potential binding interaction, antibodies raised against peptide sequences of the proposed CR2-binding site on IFNα were found to inhibit the CR2-C3d interaction in cell binding assays. It was also found that IFNα binding CR2 inhibits CR2-C3d complex formation in cell binding assays. In addition, it was found that IFNα inhibited the capping of CR2 by gp350, thus acting as an antiviral inhibitor of early phase infection from EBV (18). More recently, a biophysical study has been completed on the thermodynamic properties of CR2-ligand interactions, thus indicating the physical binding of CR2 and IFNα (17). In this study, we have moved further toward defining a binding site or binding surface for the CR2-IFNα interaction. Using NMR titration studies as before, we have determined that the following amino acids are involved in the CR2-IFNα interaction: Arg^{13}, Tyr^{16}, Arg^{28}, Ser^{42}, Lys^{48}, Lys^{50}, Tyr^{68}, Arg^{83}, Gly^{84}, and Arg^{89}.

As with other CR2-ligand interactions, the CR2-IFNα interaction is largely driven by electrostatic interactions. The CR2-IFNα interaction is likely the closest related to the C3d interaction, which makes sense because the proposed CR2-binding motifs of C3d and IFNα are the closest. In addition, the same linker region residue, Tyr^{68}, appears to undergo significant per-

TABLE 2

CR2-ligand binding residues

Shown are residues involved in each CR2-ligand binding interaction. Residues with an asterisk are unique to the respective binding interaction.

CR2-C3d	CR2-gp350	CR2-IFNα
Ile^{9*}		
	Asn^{11*}	
Arg^{13}	Arg^{13}	Arg^{13}
Tyr^{16}		Tyr^{16}
Ala^{22}	Ala^{22}	
Arg^{28}	Arg^{28}	Arg^{28}
Tyr^{29*}		
Cys^{31*}		
Ser^{32}	Ser^{32}	
Gly^{33*}		
Thr^{34*}		
	Arg^{36*}	
	Lys^{41*}	
		Ser^{42*}
Lys^{48}		Lys^{48}
		Lys^{50*}
Asp^{56*}		
Lys^{57}	Lys^{57}	
	Tyr^{64*}	
	Lys^{57*}	
Tyr^{68}	Tyr^{68}	Tyr^{68}
Ser^{70*}		
Arg^{83}	Arg^{83}	Arg^{83}
Gly^{84}	Gly^{84}	Gly^{84}
Arg^{89}	Arg^{89}	Arg^{89}
His^{90*}		
Asp^{92*}		
Ser^{93*}		
Ala^{97*}		
Thr^{100*}		
Asn^{101*}		
Ser^{109*}		
Ser^{128*}		

turbations upon addition of either C3d and IFNα, as well as the same overall layout of residues involved in both interactions (Fig. 4*C*).

Thermodynamic studies of CR2-ligand interactions have yielded slightly differing results (Table 2). As reported previously, the CR2-C3d interaction has been described as either being a two-site or a single site binding interaction (17, 48). Our ITC data best fit a two-mode binding model with a weaker K_d of 160 μM and a tighter interaction of 0.13 μM. This K_d value is fairly close to the previously determined K_d value from a surface plasmon resonance-based biophysical study (17). Using ITC, we are now able for the first time to measure in the fluid phase the two separate affinities for the two unique binding events. The CR2-C3d interaction is unique in that all other characterized CR2-ligand interactions fit a simple one to one binding isotherm. In contrast, our current ITC study of the CR2-gp350 interaction best fit a single binding isotherm with a K_d of 0.014 μM, and this affinity is only slightly tighter than the previously reported surface plasmon resonance-based K_d of 0.077 μM. The difference in affinities here could be due to the differing experimental conditions of the respective studies. Finally, our investigation of the thermodynamic properties of the CR2-IFNα interaction best fit a single binding isotherm with a K_d of 0.036 μM, and this affinity is again in excellent agreement with the previously reported surface plasmon resonance-derived K_d of 0.042 μM. Again, the likely difference is due to the difference in buffers used as well as due to the physical nature differences of each assay, one being purely in solution and the other has CR2 fixed to a solid support. The rank order of binding strength makes sense in that both IFNα and gp350 binding inhibits C3d binding to CR2, which has been reported previously (17, 18).

In summary, our continued approach to map the CR2 ligand-binding residues has yielded two new binding maps for the CR2 ligands gp350 and IFNα. We have shown that the gp350-binding site on CR2 consists mainly of SCR1 and the inter-SCR linker domains. Of the three ligand-binding sites on CR2 that we have been able to characterize in this and a previous study (48), the gp350-binding site residues are the most different of the three other characterized ligands. More similar to the C3d-binding site is that of the IFNα-binding site on CR2. Fig. 4*C*, a binding map summary that illustrates unique amino acids as well as the six shared amino acids, allows one to envision how each ligand binds in respect to the others. Examining more closely the three ligation state chemical shift change magnitudes also demonstrates the differential ligand binding ability of CR2 (Fig. 3). In addition to characterizing the binding sites for gp350 and IFNα on CR2, we have been able to carry out a thermodynamic study of the CR2-C3d, CR2-gp350, and CR2-IFNα interactions. CR2-gp350 has the tightest interaction followed closely by the CR2-IFNα interaction, with the CR2-C3d interaction being the weakest. Furthermore, we have shown that the CR2-C3d interaction is very likely a two-mode binding process.

REFERENCES

1. Fingeroth, J. D., Clabby, M. L., and Strominger, J. D. (1988) *J. Virol.* **62,** 1442–1447
2. Fujisaku, A., Harley, J. B., Frank, M. B., Gruner, B. A., Frazier, B., and Holers, V. M. (1989) *J. Biol. Chem.* **264,** 2118–2125
3. Moore, M. D., Cooper, N. R., Tack, B. F., and Nemerow, G. R. (1987) *Proc. Natl. Acad. Sci. U.S.A.* **84,** 9194–9198
4. Weis, J. J., Fearon, D. T., Klickstein, L. B., Wong, W. W., Richards, S. A., de Bruyn Kops, A., Smith, J. A., and Weis, J. H. (1986) *Proc. Natl. Acad. Sci. U.S.A.* **83,** 5639–5643
5. Weis, J. J., Toothaker, L. E., Smith, J. A., Weis, J. H., and Fearon, D. T. (1988) *J. Exp. Med.* **167,** 1047–1066
6. Ahearn, J. M., and Fearon, D. T. (1989) *Adv. Immunol.* **46,** 183–219
7. Cooper, N. R., Moore, M. D., and Nemerow, G. R. (1988) *Annu. Rev. Immunol.* **6,** 85–113
8. Holers, V. M. (1995) *Principles and Practices of Clinical Immunology* (Rich, R., ed) pp. 363–391, Mosby, St. Louis
9. Tolnay, M., and Tsokos, G. C. (1998) *Clin. Immunol. Immunopathol.* **88,** 123–132
10. Iida, K., Nadler, L., and Nussenzweig, V. (1983) *J. Exp. Med.* **158,** 1021–1033
11. Weis, J. J., Tedder, T. F., and Fearon, D. T. (1984) *Proc. Natl. Acad. Sci. U.S.A.* **81,** 881–885
12. Fingeroth, J. D., Weis, J. J., Tedder, T. F., Strominger, J. L., Biro, P. A., and Fearon, D. T. (1984) *Proc. Natl. Acad. Sci. U.S.A.* **81,** 4510–4514
13. Nemerow, G. R., Houghten, R. A., Moore, M. D., and Cooper, N. R. (1989) *Cell* **56,** 369–377
14. Nemerow, G. R., Wolfert, R., McNaughton, M. E., and Cooper, N. R. (1985) *J. Virol.* **55,** 347–351
15. Aubry, J. P., Pochon, S., Gauchat, J. F., Nueda-Marin, A., Holers, V. M., Graber, P., Siegfried, C., and Bonnefoy, J. Y. (1994) *J. Immunol.* **152,** 5806–5813
16. Aubry, J. P., Pochon, S., Graber, P., Jansen, K. U., and Bonnefoy, J. Y. (1992) *Nature* **358,** 505–507
17. Asokan, R., Hua, J., Young, K. A., Gould, H. J., Hannan, J. P., Kraus, D. M., Szakonyi, G., Grundy, G. J., Chen, X. S., Crow, M. K., and Holers, V. M. (2006) *J. Immunol.* **177,** 383–394
18. Delcayre, A. X., Lotz, M., and Lernhardt, W. (1993) *J. Virol.* **67,** 2918–2921
19. Delcayre, A. X., Salas, F., Mathur, S., Kovats, K., Lotz, M., and Lernhardt, W. (1991) *EMBO J.* **10,** 919–926

20. Martin, D. R., Yuryev, A., Kalli, K. R., Fearon, D. T., and Ahearn, J. M. (1991) *J. Exp. Med.* **174,** 1299–1311
21. Tuveson, D. A., Ahearn, J. M., Matsumoto, A. K., and Fearon, D. T. (1991) *J. Exp. Med.* **173,** 1083–1089
22. Bohnsack, J. F., and Cooper, N. R. (1988) *J. Immunol.* **141,** 2569–2576
23. Carter, R. H., and Fearon, D. T. (1989) *J. Immunol.* **143,** 1755–1760
24. Carter, R. H., and Fearon, D. T. (1992) *Science* **256,** 105–107
25. Carter, R. H., Spycher, M. O., Ng, Y. C., Hoffman, R., and Fearon, D. T. (1988) *J. Immunol.* **141,** 457–463
26. Dempsey, P. W., Allison, M. E., Akkaraju, S., Goodnow, C. C., and Fearon, D. T. (1996) *Science* **271,** 348–350
27. Luxembourg, A. T., and Cooper, N. R. (1994) *J. Immunol.* **153,** 4448–4457
28. Lyubchenko, T., dal Porto, J., Cambier, J. C., and Holers, V. M. (2005) *J. Immunol.* **174,** 3264–3272
29. Ahearn, J. M., Hayward, S. D., Hickey, J. C., and Fearon, D. T. (1988) *Proc. Natl. Acad. Sci. U.S.A.* **85,** 9307–9311
30. Tanner, J., Weis, J., Fearon, D., Whang, Y., and Kieff, E. (1987) *Cell* **50,** 203–213
31. Lowell, C. A., Klickstein, L. B., Carter, R. H., Mitchell, J. A., Fearon, D. T., and Ahearn, J. M. (1989) *J. Exp. Med.* **170,** 1931–1946
32. Moore, M. D., DiScipio, R. G., Cooper, N. R., and Nemerow, G. R. (1989) *J. Biol. Chem.* **264,** 20576–20582
33. Nemerow, G. R., Mold, C., Schwend, V. K., Tollefson, V., and Cooper, N. R. (1987) *J. Virol.* **61,** 1416–1420
34. Mullen, M. M., Haan, K. M., Longnecker, R., and Jardetzky, T. S. (2002) *Mol. Cell* **9,** 375–385
35. Spriggs, M. K., Armitage, R. J., Comeau, M. R., Strockbine, L., Farrah, T., Macduff, B., Ulrich, D., Alderson, M. R., Müllberg, J., and Cohen, J. I. (1996) *J. Virol.* **70,** 5557–5563
36. Haan, K. M., Lee, S. K., and Longnecker, R. (2001) *Virology* **290,** 106–114
37. Haddad, R. S., and Hutt-Fletcher, L. M. (1989) *J. Virol.* **63,** 4998–5005
38. Molesworth, S. J., Lake, C. M., Borza, C. M., Turk, S. M., and Hutt-Fletcher, L. M. (2000) *J. Virol.* **74,** 6324–6332
39. Baechler, E. C., Batliwalla, F. M., Karypis, G., Gaffney, P. M., Ortmann, W. A., Espe, K. J., Shark, K. B., Grande, W. J., Hughes, K. M., Kapur, V., Gregersen, P. K., and Behrens, T. W. (2003) *Proc. Natl. Acad. Sci. U.S.A.* **100,** 2610–2615
40. Santiago-Raber, M. L., Baccala, R., Haraldsson, K. M., Choubey, D., Stewart, T. A., Kono, D. H., and Theofilopoulos, A. N. (2003) *J. Exp. Med.* **197,** 777–788
41. Takahashi, K., Kozono, Y., Waldschmidt, T. J., Berthiaume, D., Quigg, R. J., Baron, A., and Holers, V. M. (1997) *J. Immunol.* **159,** 1557–1569
42. Young, K. A., Chen, X. S., Holers, V. M., and Hannan, J. P. (2007) *J. Biol. Chem.* **282,** 36614–36625
43. Young, K. A., Herbert, A. P., Barlow, P. N., Holers, V. M., and Hannan, J. P. (2008) *J. Virol.* **82,** 11217–11227
44. Dominguez, C., Boelens, R., and Bonvin, A. M. (2003) *J. Am. Chem. Soc.* **125,** 1731–1737
45. Szakonyi, G., Klein, M. G., Hannan, J. P., Young, K. A., Ma, R. Z., Asokan, R., Holers, V. M., and Chen, X. S. (2006) *Nat. Struct. Mol. Biol.* **13,** 996–1001
46. Guthridge, J. M., Rakstang, J. K., Young, K. A., Hinshelwood, J., Aslam, M., Robertson, A., Gipson, M. G., Sarrias, M. R., Moore, W. T., Meagher, M., Karp, D., Lambris, J. D., Perkins, S. J., and Holers, V. M. (2001) *Biochemistry* **40,** 5931–5941
47. Hannan, J. P., Young, K. A., Guthridge, J. M., Asokan, R., Szakonyi, G., Chen, X. S., and Holers, V. M. (2005) *J. Mol. Biol.* **346,** 845–858
48. Kovacs, J. M., Hannan, J. P., Eisenmesser, E. Z., and Holers, V. M. (2009) *J. Biol. Chem.* **284,** 9513–9520
49. Pervushin, K., Riek, R., Wider, G., and Wüthrich, K. (1997) *Proc. Natl. Acad. Sci. U.S.A.* **94,** 12366–12371
50. Wittkekind, M., and Mueller, L. (1993) *J. Magn. Reson.* **101,** 201–205
51. Grzesiek, S., and Bax, A. (1992) *J. Magn. Reson.* **96,** 432–440
52. Zuiderweg, E. R., and Fesik, S. W. (1989) *Biochemistry* **28,** 2387–2391
53. Delaglio, F., Grzesiek, S., Vuister, G. W., Zhu, G., Pfeifer, J., and Bax, A. (1995) *J. Biomol. NMR* **6,** 277–293
54. Vranken, W. F., Boucher, W., Stevens, T. J., Fogh, R. H., Pajon, A., Llinas, M., Ulrich, E. L., Markley, J. L., Ionides, J., and Laue, E. D. (2005) *Proteins* **59,** 687–696
55. Wiseman, T., Williston, S., Brandts, J. F., and Lin, L. N. (1989) *Anal. Biochem.* **179,** 131–137
56. Carel, J. C., Myones, B. L., Frazier, B., and Holers, V. M. (1990) *J. Biol. Chem.* **265,** 12293–12299
57. Prota, A. E., Sage, D. R., Stehle, T., and Fingeroth, J. D. (2002) *Proc. Natl. Acad. Sci. U.S.A.* **99,** 10641–10646
58. Molina, H., Brenner, C., Jacobi, S., Gorka, J., Carel, J. C., Kinoshita, T., and Holers, V. M. (1991) *J. Biol. Chem.* **266,** 12173–12179
59. Morikis, D., and Lambris, J. D. (2004) *J. Immunol.* **172,** 7537–7547
60. Zhang, L., Mallik, B., and Morikis, D. (2007) *J. Mol. Biol.* **369,** 567–583